Proceedings of the 17th World Congress
The International Federation of Automatic Control
Seoul, Korea, July 6-11, 2008

Relative State Estimation of Satellite Formation Flying Using Kalman Filter

Young-Gu Lee*, Hyochoong Bang**

***School of Mechanical, Aerospace & Systems Engineering, Department of Aerospace Engineering, KAIST Daejeon, Korea, (Tel: 82-42-869-3789; e-mail: yglee@fdcl.kaist.ac.kr).**
**** School of Mechanical, Aerospace & Systems Engineering, Department of Aerospace Engineering, KAIST Daejeon, Korea, (Tel: 82-42-869-3722; e-mail:hcbang@fdcl.kaist.ac.kr).**

Abstract: In this paper, an approach is proposed for relative state estimation for satellites in formation flying. To estimate the relative states of two satellites, the Kalman Filter algorithms (EKF, UKF) are adopted with the relative range and range rate between two satellites and attitude of a satellite as measurement variables. In case that the initial state and measurements errors are moderate, both EKF and UKF perform well. As those errors increase, however, the EKF degrades unlike the UKF. Numerical simulations are performed under two circumstances. The first one presented both chief and deputy satellites are orbiting a circular reference orbit around a perfectly spherical Earth model with no disturbing acceleration, in which the elementary relative orbital dynamics are taken into account. In reality however, the Earth is not a perfect sphere, but rather an oblate spheroid. Both satellites are under the effect of J_2 geopotential disturbance, which causes the relative distance between two satellites to increase gradually. The near-Earth orbit decays as a result of atmospheric drag. In order to remove the modeling error, the second scenario incorporates the effect of J_2 geopotential disturbing force, atmospheric drag, and the eccentricity.

1. INTRODUCTION

In many future space mission designs, satellite formation flying technology will be applied to the areas such as stereographic imaging, long baseline interferometery, and synthetic aperture radar (SAR). Formation flying contains advantages of structural flexibility in that even when one of the satellites which form the cluster fails, the mission can be carried out by reconfiguring the rest of the them, and the fine economical feasibility in that multiple satellites can provide a large size of aperture of radar dish without attempting to build up a large size radar dish by way of forming a formation with its radius ranging from several meters to kilometres. Recently the global positioning system (GPS) is adopted to measure the relative position among satellites, but these systems are applicable only to near-Earth orbiting satellites and are subjected to its deficiencies such as geometric dilution of precision, and multipath. Some papers made use of a vision-based navigation (VISNAV) system, which provides line-of-sight (LOS) vectors between two satellites as a relative sensor measurement to surmount the drawback of GPS. In this paper, however, relative distance and speed between two satellites, and satellite's attitude are adopted for relative sensor measurement. With such information the Kalman filter algorithms (EKF, UKF) are implemented to estimate the system state. This paper consists of an overview of the relative orbit dynamics of two satellites with/without the effects of J_2 disturbing force, atmospheric drag, and eccentricity of orbit, and the estimation of relative state variables using the Kalman filter algorithms. Finally, the simulation results are presented.

2. RELATIVE ORBIT DYNAMICS

2.1 The Hill-Clohessy-Wiltshire equations

The chief satellite is the one about which all other satellites are orbiting. The remaining satellites referred to as the deputy satellites, are orbiting the chief and constitute a formation with the chief as their center. The equations of relative motion are derived under the assumptions that the chief orbit is circular, the relative distance between the chief and deputy satellites is small compared with the chief orbit radius, the Earth is perfectly sphere and homogeneous, and there is no force acting on the two bodies other than the inverse-squared gravitational force. The relative motion of satellites are described in terms of Cartesian coordinates vector in the chief satellite-centered rotating reference frame, referred to as Hill frame with its vector components $\{o_r, o_\theta, o_h\}$,

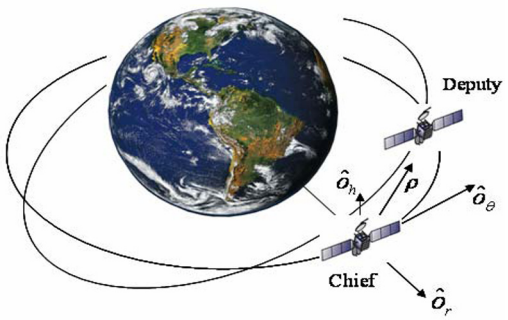

Fig. 1. Illustration of the Hill's frame

where o_r is in the orbit radius direction, o_θ is in along track direction, and o_h completes a vector triad.

$$\rho = (x, y, z)^T \tag{1}$$

The deputy satellite position vector can be expressed as

$$r_d = r_c + \rho = (r_c + x)\hat{o}_r + y\hat{o}_\theta + z\hat{o}_h \tag{2}$$

where r_c and r_d are the inertial chief and deputy position vectors, respectively. The acceleration vector of the chief satellite, taking the second derivatives with respect to the inertial frame, is given by

$$\ddot{\vec{r}}_c = (\ddot{r}_c - r_c \dot{f}^2)\hat{o}_r = -\frac{\mu}{r_c^3}\vec{r}_c = -\frac{\mu}{r_c^2}\hat{o}_r \tag{3}$$

Because the chief orbit angular momentum magnitude can be expressed as $h = r_c^2 \dot{f}$ and h is constant for unperturbed case, taking derivative of h with respect to time yields

$$\begin{aligned} \dot{h} &= 2r_c \dot{r}_c \dot{f} + r_c^2 \ddot{f} = 0 \\ \ddot{f} &= -2\frac{\dot{r}}{r_c}\dot{f} \end{aligned} \tag{4}$$

From Eqs. (2), (3), and (4), the acceleration vector of the deputy satellite can be expressed as

$$\begin{aligned} \ddot{r}_d = &[\ddot{x} - 2\dot{f}(\dot{y} - y\frac{\dot{r}}{r_c}) - x\dot{f}^2 - \frac{\mu}{r_c^2}]\hat{o}_r \\ &+ [\ddot{y} + 2\dot{f}(\dot{x} - x\frac{\dot{r}}{r_c}) - y\dot{f}^2]\hat{o}_\theta + \ddot{z}\hat{o}_h \end{aligned} \tag{5}$$

If the relative distance between the chief and the deputy satellites is small compared with the chief orbit radius, then the relative orbit equations of motion are described as

$$\begin{aligned} &\ddot{x} - x\dot{f}^2(1 + 2\frac{r_c}{p}) - 2\dot{f}(\dot{y} - y\frac{\dot{r}_c}{r_c}) = 0 \\ &\ddot{y} - y\dot{f}^2(1 - \frac{r_c}{p}) + 2\dot{f}(\dot{x} - x\frac{\dot{r}}{r_c}) = 0 \\ &\ddot{z} + \frac{r_c}{p}\dot{f}^2 z = 0 \end{aligned} \tag{6}$$

where f is true anomaly and p is the semilatus rectum of the chief satellite. It is referred to the literature [Schaub and Junkins 2003] for further details. If the chief orbit is chosen to be circular, then the well-known Hill-Clohessy-Wiltshire (HCW) equations are given by

$$\begin{aligned} &\ddot{x} - 2n\dot{y} - 3n^2 x = 0 \\ &\ddot{y} - 2\,n\dot{x} = 0 \\ &\ddot{z} + n^2 z = 0 \end{aligned} \tag{7}$$

where n represents the mean orbital rate of the chief satellite.

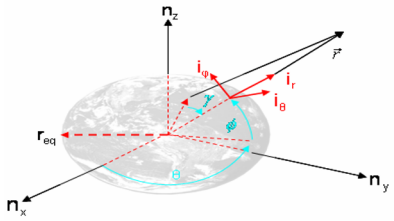

Fig. 2. Illustration of Gravitational Potential

2.2 The J_2 modified HCW equations

The HCW equations derived in the previous section are based on the assumption that the Earth is perfectly sphere and its mass distribution is homogeneous. In reality, however, it is not true. In this section, we take the effect of J_2 on relative orbit dynamics into account by adding the J_2 induced gravitational acceleration to the right side of the HCW equations as a forcing term [Schweighart et al 2001]. The gravitational potential of the earth, accounting for only latitude variation, takes on the following

$$V = -\frac{Gm}{r}\left[1 - \sum_{k=2}^{\infty}\left(\frac{r_{eq}}{r}\right)^k J_k P_k(\sin\phi)\right] \tag{8}$$

where r_{eq} denotes the radius of the earth at its equator, the P_k refer to the Legendre polynomial functions of order k. The J_k are constant coefficients, and ϕ is the geocentric latitude. From Fig. 2 it is evident that $\sin\phi = \frac{z}{r}$. Hence, the disturbing potential in spherical coordinates caused by J_2 is given by

$$\begin{aligned} V_{J_2} &= \frac{\mu}{2r}\left(\frac{r_{eq}}{r}\right)^2 J_2(1 - 3\sin^2 i \sin^2\theta) \\ &= \frac{\mu}{2r}\left(\frac{r_{eq}}{r}\right)^2 J_2[1 - 3\left(\frac{z}{r}\right)^2] \end{aligned} \tag{9}$$

The J_2 induced gravitational acceleration acting on a satellite can be derived by taking partial derivative and transforming coordinates from the inertial frame to the LVLH frame using the direction cosine matrix

$$a_{J_2} = -\frac{3\mu r_{eq}^2}{2r^4} J_2 \begin{bmatrix} 1 - 3\sin^2 i \sin^2\theta) \\ 2\sin^2 i \sin\theta\cos\theta \\ 2\sin i \cos i \sin\theta \end{bmatrix} \tag{10}$$

Application of Eq. (10) into Eq. (7) brings forth the following equations;

$$\begin{aligned} &\ddot{x} - 2n\dot{y} - 3n^2 x = -k(1 - 3\sin^2 i \sin^2\theta) \\ &\ddot{y} - 2\,n\dot{x} = -2k\sin^2 i \sin\theta\cos\theta \\ &\ddot{z} + n^2 z = -2k\sin i \cos i \sin\theta \end{aligned} \tag{11}$$

where $k = \frac{3\mu r_{eq}^2}{2r^4} J_2$ and $n = \sqrt{\frac{\mu}{r^3}}$.

2.3 The modified HCW equations accommodating Atmospheric Drag

In this section we take the effects of atmospheric drag on the satellites formation into account. The previous works done by [Carter and Humi 2002] will be reviewed and applied as system dynamics for estimating the relative state between two satellites in the following section. In the inertial frame the equations of motion of a satellite can be expressed as

$$\ddot{r}_c = -f(r_c)r_c - \alpha g(r_c)\left|\dot{r}_c\right|\dot{r}_c \tag{12}$$

The first term on the right hand side accounts for gravitational acceleration due to a central force field and the second indicates atmospheric drag acceleration. The scalar α is a constant associated with the atmospheric drag coefficient and the geometry of the satellite. The function g is atmospheric density, which is dependent only on altitude. Equation (12) can be rewritten as

$$\ddot{r}_c = -f(r_c)r_c - \alpha g(r_c)r_c\dot{\theta}\dot{r}_c \tag{13}$$

under the assumption that the orbit is initially not of high eccentricity but decays due to drag, in which the magnitude of the radial velocity is very small compared with that of the transverse velocity, that is, $\left|\dot{r}_c\right| << r_c\dot{\theta}$. In the same way the motion of the deputy satellite is governed by

$$\ddot{r}_d = -f(r_d)r_d - \beta g(r_d)r_d\dot{\phi}\dot{r}_d \tag{14}$$

where $r_d = r_c + r$ and r is the relative position vector between the chief and the deputy satellites, and β is the atmospheric drag constant associated with the deputy. $\dot{\phi}$ is the angular rate of the deputy in orbit. Transforming into a rotating frame and changing independent variables from time to the chief satellite's true anomaly with some algebraic processes lead to a simpler form such that

$$\begin{aligned} x'' &= 2y' - [f'(r_c)r_c/\omega^2 + \alpha g(r_c)r_c' + \beta g'(r_c)r_c r_c' \\ &\quad -(\beta-\alpha)g(r_c)[(r_c x)' + r_c' x - r_c y + r_c r_c'/E(\theta)] \\ y'' &= -2x' - r_c[\alpha g(r_c) + \beta g'(r_c)r_c]y \\ &\quad -(\beta-\alpha)g(r_c)[2r_c y + (r_c y)' + r_c^2 E(\theta)] \\ z'' &= -z - (r_c z)'(\beta-\alpha)g(r_c) \end{aligned} \tag{15}$$

where $E(\theta)$ is a transformation for simplifying the governing equations, and further details are given in the reference. In Newtonian gravitational field, $f(r_c) = \mu/r_c^3$ and $g(r_c) = 1/r_c$. The acceleration due to the atmospheric drag is, therefore, $-(\alpha/r_c)\left|\dot{r}_c\right|\dot{r}_c$. Under the assumption that the chief and the deputy satellites are close enough to each other, they have identical drag constants, i.e., $\alpha = \beta$. Therefore, we are led to the following elegant form

$$\begin{aligned} x'' &= 2y' + \frac{3(1+4\alpha^2)x}{1+\varepsilon e^{-2\alpha\theta}\cos(\theta-\theta_0)} \\ y'' &= -2x' \\ z'' &= -z \end{aligned} \tag{16}$$

where ε is eccentricity of the chief satellite.

3. RELATIVE STATE ESTIMATION

In this section, estimation of the relative state between two satellites will be presented using EKF and UKF as estimators. Neither of the estimators is new. Both can be found in the several literature and text books (for instance, Juilier and Uhlmann 1995).

3.1 EKF State Estimation

From given system dynamic and measurement models, we would like to obtain the minimum mean squared error(MMSE) estimate of the system state vector. The EKF makes use of linearized system dynamics and measurement models, assuming that the nonlinearity in system and measurement models is sufficiently smooth and small. To obtain the MMSE, the EKF is applied to the nonlinear discrete time system of the form

$$\begin{aligned} x(k+1) &= f[x(k), v(k), k], \\ z(k) &= h[x(k), k] + w(k) \end{aligned} \tag{17}$$

where $x(k)$ is the state of the system at time step k, $v(k)$ is the system noise, $z(k)$ is the measurement vector, and $w(k)$ is the measurement noise. The control input is not considered here. It is assumed that all the noises are zero-mean white Gaussian and there is no correlation between them.

$$\begin{aligned} &E[v(i)v^T(j)] = \delta_{ij}Q(i), \\ &E[w(i)w^T(j)] = \delta_{ij}R(i), \\ &E[v(i)w^T(j)] = 0, \ \ for\ all\ i, j \end{aligned} \tag{18}$$

where Q and R represent the covariance of system noise and measurement noise, respectively. The problem of determining the MMSE is equivalent to computing the conditional mean from given measurements. The EKF propagates the first two moments of the distribution of $x(k)$, mean and covariance, through the system and measurement equations, recursively, and then the transformed mean and covariance are updated with a new current measurement. To sum up,

1) Predicted quantities at time step k

$$\begin{aligned} &\hat{x}(k+1\,|\,k) = f[\hat{x}(k\,|\,k), k+1], \\ &P(k+1\,|\,k) = J_f P(k\,|\,k)J_f^T + Q(k+1) \\ &\hat{z}(k+1\,|\,k) = h[\hat{x}(k\,|\,k), k+1], \\ &P_{vv}(k+1\,|\,k) = J_h P(k+1\,|\,k)J_h^T + R(k+1) \end{aligned} \tag{19}$$

where J_f and J_h, P_{vv} denote the Jacobian matrices of the process and measurement models, and the predicted measurement covariance, respectively.

2) Estimated quantities at time step $k+1$ with a new current measurement at time step $k+1$

$$\begin{aligned}
&\hat{x}(k+1|k+1) = \hat{x}(k+1|k) + W(k+1)v(k+1) \\
&P(k+1|k+1) = P(k+1|k) - W(k+1)P_{vv}(k+1|k)W(k+1) \\
&v(k+1) = z(k+1) - \hat{z}(k+1|k) \\
&W(k+1) = P_{xv}(k+1|k)P_{vv}^{-1}(k+1|k)
\end{aligned} \tag{20}$$

where $W(k+1), v(k+1)$, and P_{xv} represent the Kalman gain, the discrepancy between the actual measurement and the predicted measurement, and the cross-covariance, respectively. In this paper, the relative distance, speed, and attitude of the chief satellite are to be used as measurements to estimate the relative state. Fig. 3 shows the illustration of the measurement geometry between two satellites.

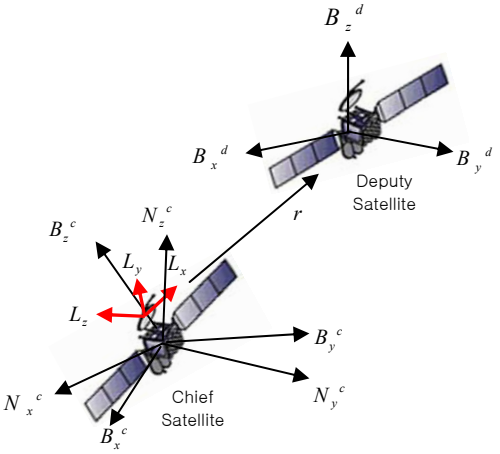

Fig. 3. Illustration of Measurement Geometry between two satellites

N^c, B^c, B^d, and L denote the LVLH frame, chief satellite's body frame, deputy satellite's body frame, and the sensor frame, respectively. We assume that the origins of N^c, B^c, and L frames coincide with each other assuming that the offset distance of the laser range finder from the origin of the chief satellite is small enough compared to the relative distance between two satellite. The relative position vector between the two satellites can be obtained through the coordinate transformation, which makes use of the relative distance and the attitude of the chief satellite equipped with a laser range finder.

$$R^{LVLH} = C_{B_c}^{LVLH} C_L^{B_c} \begin{vmatrix} r \\ 0 \\ 0 \end{vmatrix}^L \tag{21}$$

where $C_{B_c}^{LVLH}$ and $C_L^{B_c}$ represent the rotational matrices which convert a vector expressed in the chief satellite's body frame to a vector expressed in the LVLH frame, and convert a vector expressed in the sensor frame to a vector expressed in the chief satellite's body frame, respectively. Furthermore, R^{LVLH} and r denote the relative position vector between two satellites expressed in the LVLH frame and relative distance measured from the laser range finder, respectively. We assume that the laser range finder is aligned along the x-axis of the sensor frame, and the attitude of the chief satellite with respect to the LVLH frame is known very accurately to the extent of 0.0001 degree from the secondary attitude measuring devices such as star sensor. The relative position vector obtained in (21) suffices to estimate the relative state, however, for the sake of improved observability we adopt relative speed as additional measurement, which is obtained from a Doppler radar. The measurement vector is given by

$$h_{4\times1} = [R_{3\times1}^{LVLH^T} \quad \dot{\rho}_{1\times1}]^T \tag{22}$$

where $\dot{\rho} = (x\dot{x} + y\dot{y} + z\dot{z})/\rho$ represents the relative range rate. Note that the measurement vector is originally linear, but becomes nonlinear due to the augmented additional measurement. Taking the partial derivative of the measurement vector with respect to the state yields the output sensitivity equations as

$$\left.\frac{\partial h}{\partial x}\right|_{x=\hat{x}_k} = \begin{bmatrix} 1 & 0 & 0 & 0 & 0 & 0 \\ 0 & 1 & 0 & 0 & 0 & 0 \\ 0 & 0 & 1 & 0 & 0 & 0 \\ -\frac{x\dot{\rho}}{\rho^2}+\frac{\dot{x}}{\rho} & -\frac{y\dot{\rho}}{\rho^2}+\frac{\dot{y}}{\rho} & -\frac{z\dot{\rho}}{\rho^2}+\frac{\dot{z}}{\rho} & \frac{x}{\rho} & \frac{y}{\rho} & \frac{z}{\rho} \end{bmatrix} \tag{23}$$

where $\rho = \sqrt{(x^2+y^2+z^2}$ denotes relative range between the two satellites.

3.2 UKF State Estimation

For nonlinear process and/or measurement model, however, the state distribution is approximated by a Gaussian random variable and then propagated through the first order linearized equations of system dynamics. As nonlinearity of system becomes dominant, the errors in the true posterior mean and covariance of the transformed Gaussian random variables may also become larger, deteriorating the filter performance. To overcome the linearization issue in the EKF, the UKF makes use of carefully chosen deterministic sample points called sigma points whose transformed ensemble mean and covariance capture the true mean and covariance. The sigma points are obtained as follows:

$$\begin{aligned}
&\chi_0(k|k) = \hat{x}(k|k) \quad W_0 = k/(n+k) \\
&\chi_i(k|k) = \hat{x}(k|k) + (\sqrt{(n+k)P(k|k)})_i \quad W_i = 1/(2(n+k)) \\
&\chi_{i+n}(k|k) = \hat{x}(k|k) - (\sqrt{(n+k)P(k|k)})_i \quad W_{i+n} = 1/(2(n+k))
\end{aligned} \tag{24}$$

where k is the scaling parameter for the forth and higher moments of the distribution, W_i is the weight of each point. The calculated sigma points are then passed through the nonlinear system equations to produce a set of transformed sample points. The predicted mean and covariance are calculated from the transformed sample points such that

$$\begin{aligned}
\hat{x}(k+1|k) &= \sum_{i=0}^{2n} W_i \chi_i(k+1|k) \\
P(k+1|k) &= \sum_{i=0}^{2n} W_i \{\chi_i(k+1|k) - \hat{x}(k+1|k)\} \\
&\quad \times \{\chi_i(k+1|k) - \hat{x}(k+1|k)\}^T
\end{aligned} \tag{25}$$

In a similar manner, the sigma points are transformed through the nonlinear measurement equations, then, used to calculate the mean and covariance of predicted measurements as

$$\hat{Z}(k+1|k) = \sum_{i=0}^{2n} W_i \hat{Z}_i(k+1|k)$$
$$P_{zz}(k+1|k) = \sum_{i=0}^{2n} W_i \{Z_i(k+1|k) - \hat{Z}(k+1|k)\} \quad (26)$$
$$\times \{Z_i(k+1|k) - \hat{Z}(k+1|k)\}^T$$

In summary, the Kalman filter algorithms have the structure "predictor-corrector" in common where the means and covariances of a system and a measurement are propagated using the system and measurement model, and then they are updated with new current measurement. For a linear system, the mean and covariance are exactly updated by using the Kalman filter. However, for a nonlinear case, they are approximated by using the EKF which is based on linearized model (to the first order). The UKF, however, predicts the means and covariance up to the third order for Gaussian random variables by carefully chosen deterministic sample points, which provides higher accuracy than the EKF.

4. SIMULATION RESULTS

In this section, simulation results for the satellites relative motions incorporating the effects of J_2 geopotential disturbing force, atmospheric drag, and eccentricity in the chief satellite's orbit are provided. In addition, the performance comparison between the EKF and the UKF for estimating the relative state variables with information on the relative range and the speed between two satellites, and the attitude of chief satellite are presented. The relative dynamics described in Section 2 is chosen as the system model, and the relative position vector as well as the speed prescribed in Section 3 is adopted in the measurement model for both EKF and UKF. The simulation is conducted for 2 orbit periods with an interval of 1 degree. The measurements have been used to update the *a priori* state with the same rate of system propagation. The simulation parameters including the initial state errors are described in Table 1.

Table 1. Simulation Parameters

			Simulation Parameters
Chief Satellite	Eccentricity		0.001 / 0.03
	Altitude		700 km
	Inclination		20 deg
EKF /UKF	Q		$diag[(10^{-4}/r_c)^2{}_{6\times6}]$
	R	I	$diag[(3\times10^{-5}/r_c)^2{}_{4\times4}]$
		II	$diag[(3\times10^{-4}/r_c)^2{}_{4\times4}]$
	Initial State Error	I	$[5\times10^{-3}\ \ 3\times10^{-3}\ \ 4\times10^{-3}\ \ 1\times10^{-6}\ \ 1\times10^{-6}\ \ 1\times10^{-6}]^T$
		II	$[5\times10^{-3}\ \ 3\times10^{-3}\ \ 4\times10^{-3}\ \ 1\times10^{-3}\ \ 1\times10^{-3}\ \ 1\times10^{-3}]^T$

Figs. 4~7 show the true and the estimated relative position between the chief and deputy satellites. It turns out that the applications of the EKF and the UKF to the relative state estimation with the satellite's attitude and range and the speed information as their measurements bring forth good results for moderate errors in initial states and the measurements, irrespective of the J_2 and eccentricity and atmospheric drag. For the cases of significantly large errors in measurement and initial state, however, the EKF accuracy deteriorates due to the first order linearization in the measurement equation, while the UKF still shows a good performance.

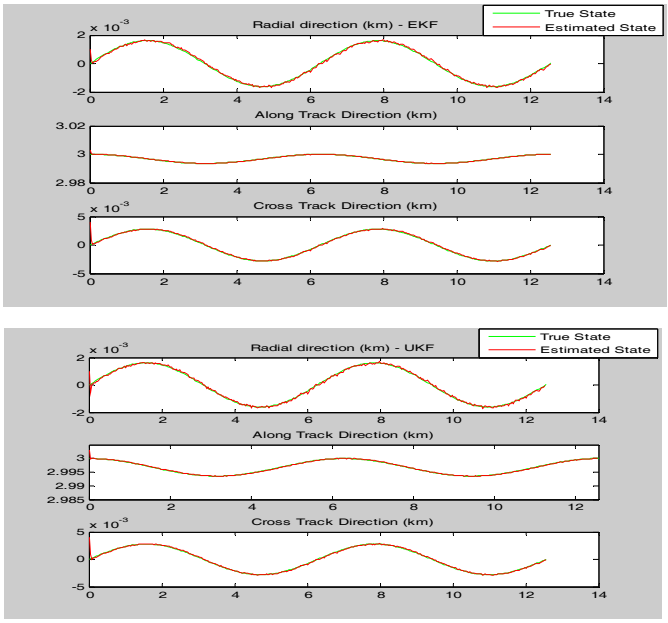

Fig. 4. True and Estimated Position with J2, atmospheric drag, and eccentricity of 0.001

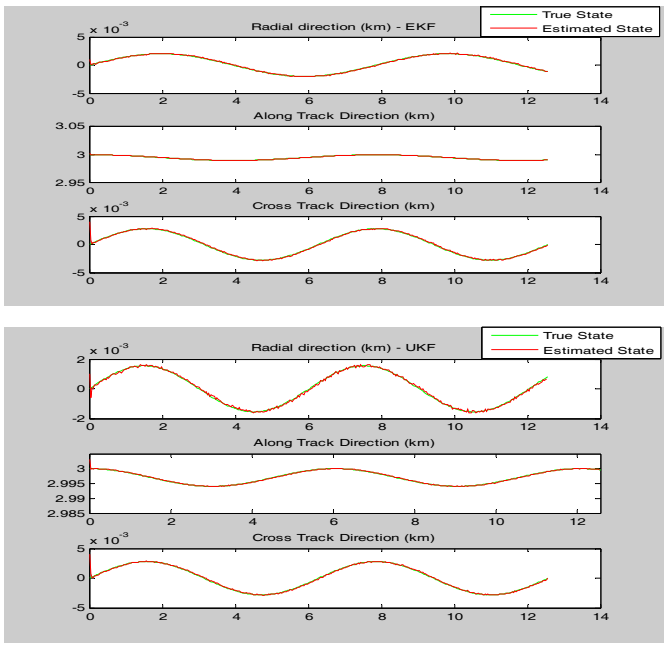

Fig. 5. True and Estimated Position with J2, atmospheric drag, and eccentricity of 0.03

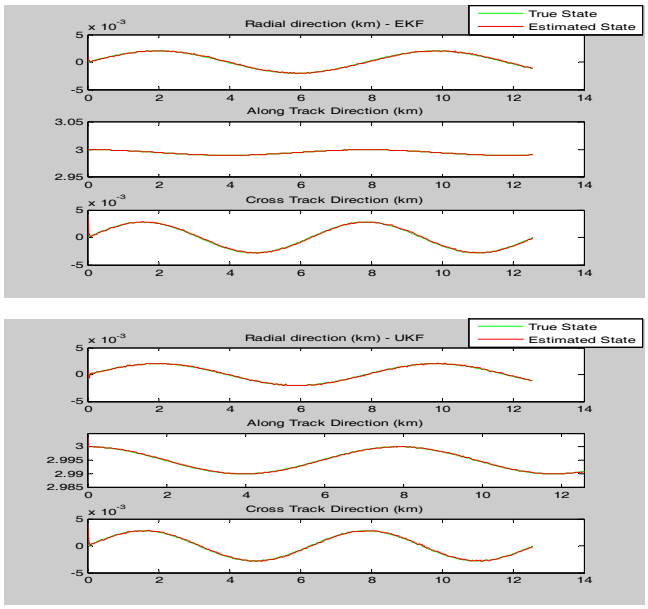

Fig. 6. True and Estimated Position with small errors in Initial State and Measurements

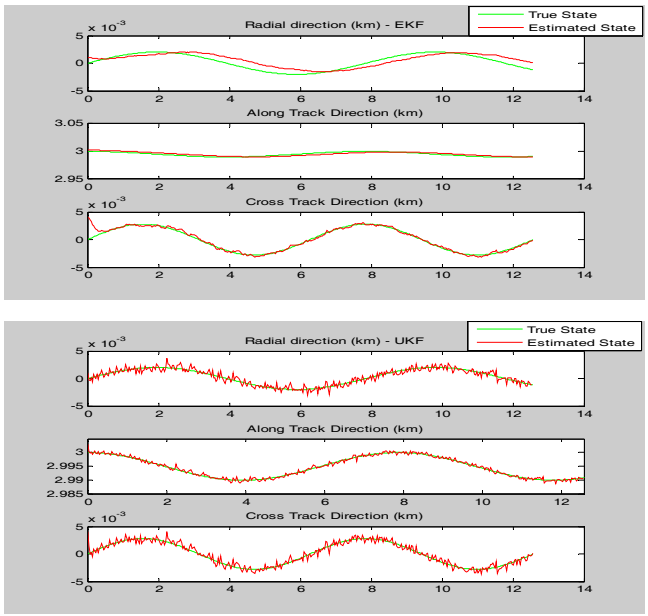

Fig. 7. True and Estimated Position with large errors in Initial State and Measurements

5. Conclusion

In this paper, the EKF and UKF algorithms are applied to the problem of estimating the relative position between two satellites, in which the measurements system proposed in our previous work [Young-Gu Lee et al. 2007], are used. Simulation results show that both the EKF and UKF have good performances within reasonable initial conditions and system parameters, using aforementioned measurement system. Furthermore, the performance comparison between two nonlinear filters (EKF and UKF) are also presented. As uncertainties in system parameters and initial conditions become larger, the UKF shows better performance.

ACKNOWLEDGEMENT

This work was supported by the Korea Science and Engineering Foundation (KOSEF) grant funded by the Korea government (MOST) (No. R01-2006-000-10189-0).

REFERENCES

Mohinder S. Grewal and Angus P. Andrews (2001). *Kalman Filtering: Theory and Practice (2nd Ed),* Wiley New York.

Richard H. Battin (1999). *An Introduction to the Mathematics and Methods of Astrodynamics*, AIAA Education Series.

Schaub, H. and Junkins, J.L. (2003). *Analytical Mechanics of Space Systems*, AIAA Educational Series.

Schweighart S. and Sedwick R. (2001). *A Perturbative Analysis of Geopotential Disturbances for Satellite Cluster Formation Flying*, IEEE Aerospace Conference, **Vol. 21**, pp. 1001-1019.

S. J. Juilier and J. K. Uhlmann (1995). A New Extension of the Kalman Filter to Nonlinear Systems, *American Control Conference*, pp. 1628-1632.

S. J. Juilier and J. K. Uhlmann. A General Method for Approximating Nonlinear Transformations of Probability Distributions, http://www.robots.ox.ac.uk/~siju

Thomas Carter, Clohessy-Wiltshire Equations Modified to Include Quadratic Drag (2002). *Journal of Guidance, Control and Dynamics* **Vol 25, No.6.**

Tshauner, J., and Hempel, P. (1965). Rendezvous zu ein Min Elliptischer Bahn Umlaufenden Ziel, *Astronautica*, **Vol. 11, No.2.**

Young-Gu Lee and Hyochoong Bang (2007). Extended Kalamn Filter Based Relative State Estimation for Satellitse in Formation Flying, *Journal of Control, Automation and Systems Engineering*, **Vol. 13, No.10.**